

STUDY OF LAMINAR CONVECTIVE HEAT TRANSFER IN HEATED CYLINDERS ROTATING INSIDE A RECTANGULAR ENCLOSURE

Paulo Mohallem Guimarães

Federal University of Itajubá
Mechanics Engineering Department
paulomgui@uol.com.br

Genésio José Menon

Federal University of Itajubá
Mechanics Engineering Department
genesio@unifei.edu.br

Abstract. *The natural convection within an enclosure with two internal heated cylinders is studied considering a two-dimensional and unsteady regime. A variety of cases is analyzed here by combining the internal cylinder temperatures and velocity directions. The Prandtl number is $Pr = 0.7$ and the Grashof number is $Gr = 10^5$. The geometry considered is a two-concentric cylinder enclosure where the outer one is cooled and rotating while the inner one does not rotate and is heated. It has also been studied here the effect of the mesh refinement. The governing equations are discretized using the finite element method with the Petrov-Galerkin perturbations and the Penalty formulation. The element used is the isoparametric quadrilateral with four nodes. A semi-implicit Euler method is used to advance in time. Indeed, a variety of results is reached here. However, one important point that is worth mentioning is that the cylinder direction is really important when high angular velocities are present and hence controlling the main flow. Some cases should be avoided when cooling is aimed, that is, the ones with high temperatures.*

Keywords: *Rotating cylinder, Natural convection, Petrov-Galerkin, Finite element method*

1. Introduction

The study of natural convection in an enclosure has been carried out for decades due to its importance in engineering applications such as solar energy systems, electronic cooling equipment, etc.

In Fu et al. (1994), a penalty finite-element numerical method is used to investigate enhancement of natural convection of an enclosure by a rotating circular cylinder near a hot wall. They conclude that the direction of the rotating cylinder plays a role in enhancing natural convection in an enclosure. In this study, the counter-clockwise rotating cylinder apparently contributes to the heat transfer rate, but the clockwise rotating cylinder does not. When the value of the Richardson number is about 103, the enhancement of the heat transfer rate begins to be revealed. The maximum enhancement of the heat transfer is approximately equal to 60%.

Nguyen et al. (1996) investigate numerically the heat transfer from a rotating circular cylinder immersed in a spatially uniform, time-dependent convective environment including the effects due to buoyancy force. The flow equations, based on the vorticity and stream function, are solved along with the energy equation by a hybrid spectral scheme that combines the Fourier spectral method in the angular direction and a spectral element method in the radial direction. Several cases are simulated for Grashof numbers up to 2×10^4 , Reynolds numbers up to 200, and a range of speed of rotation from -0.5 to $+0.5$. The results show that vortex shedding is promoted by the cylinder rotation but is vanished by the presence of the buoyancy force. In opposing flows, the counter flow currents cause a large expansion of the streamlines and isotherms in the direction normal to the free stream velocity. These changes in the structure of the flow and the temperature fields greatly modify the heat flux along the surface of the cylinder and consequently, the heat transfer rate is strongly dependent upon Reynolds number, Grashof number, rotational speed, and the gravity direction. Effects due to pulsation are also reflected in the Nusselt number history in the form of periodic oscillations.

Lee et al. make experimental investigations to study the convective phenomena of an initially stratified salt-water solution due to bottom heating in a uniformly rotating cylindrical cavity. Three types of global flow patterns initially appear depending on the effective Rayleigh number and Taylor number: stagnant flow regime, single mixed layer flow regime and multiple mixed layer flow regime. The number of layers at its initial stage and the growth height of the mixed layer decreases for the same Rayleigh number. It is ascertained in the rotating case that the fluctuation of interface between layers is weakened, the growth rate of mixed layer is retarded and the shape of interface is more regular compared to the stationary case.

Joo-Sik Yoo (1998) studies numerically the mixed convection in a horizontal concentric annulus with Prandtl number equal to 0.7. The inner cylinder is hotter than the outer cylinder. The forced flow is induced by the cold outer cylinder that rotates slowly with constant angular velocity with its axis at the center of the annulus. Investigations are made for various combinations of Rayleigh number Ra , Reynolds number Re , and ratio σ of the inner cylinder diameter to the gap width, that is, $Ra \leq 5 \times 10^4$, $Re \leq 1500$, and $0.5 \leq \sigma \leq 5$. The flow patterns can be categorized into three types according to the number of eddies: two-one- and no-eddy flows. The transitional Reynolds number between two-and

one-eddy flows for small Rayleigh number is not greatly affected by the geometrical parameter σ . Net circulation of fluid in the direction of cylinder's rotation is decreased as Ra is increased. As the speed of the cylinder's rotation is increased, the points of maximum and minimum local heat fluxes at both of the inner and outer cylinders move in the same direction of cylinder's rotation for small Ra , but for high Ra the points at the inner cylinder do not always move in the same direction. Overall heat transfer at the wall is rapidly decreased, as Re approaches the transitional Re between two- and one-eddy flows.

Lin and Yan (2000) conducted an experimental study through temperature measurements to investigate the thermal features induced by the interaction between the thermal buoyancy and rotation-induced Coriolis force and centrifugal force in an air-filled heated inclined cylinder rotating about its axis. Results are obtained ranging the thermal Rayleigh number, the Taylor number, the rotational Rayleigh number, and the inclined angle. The experimental data suggest that when the cylinder is stationary, the thermal buoyancy driven flow is random oscillation at small amplitude after initial transient for inclined angle smaller than 60° . Rotating the cylinder is found to destabilize the temperature field when the rotation speed is less than 30 rpm and to stabilize it when the rotation speed exceeds 30 rpm. Moreover, the distributions of time-average temperature in the Z -direction for various inclined angles become widely separate only at low rotation rates less than 60 rpm.

The natural convection within an enclosure with two internal heated cylinders considering the regime two-dimensional and unsteady is studied. A variety of cases is observed here by combining the cylinder temperatures and velocity directions. The Prandtl number is $Pr = 0.7$ and the Grashof number is $Gr = 10^5$ throughout this paper.

2. Problem description

The geometry and boundary conditions studied in this work are presented in Fig. 1. It is a horizontal rectangular enclosure with length W and height L . The horizontal walls are isolated while the vertical walls are kept at constant cold and hot temperatures, T_c and T_h , respectively. The internal cylinders with radius r are spaced from each other of d and equally distant from the vertical and horizontal walls. Cylinder 1 (C1) and cylinder 2 (C2) have temperatures T_1 and T_2 , respectively, and angular velocity ω . The cases studied here are a combination of the directions of ω and T_1 and T_2 which is shown later on this paper. After non-dimensionalization, L , W , r , and d will be considered to have the values 1, 2, 0.1, and 1, respectively, throughout this paper.

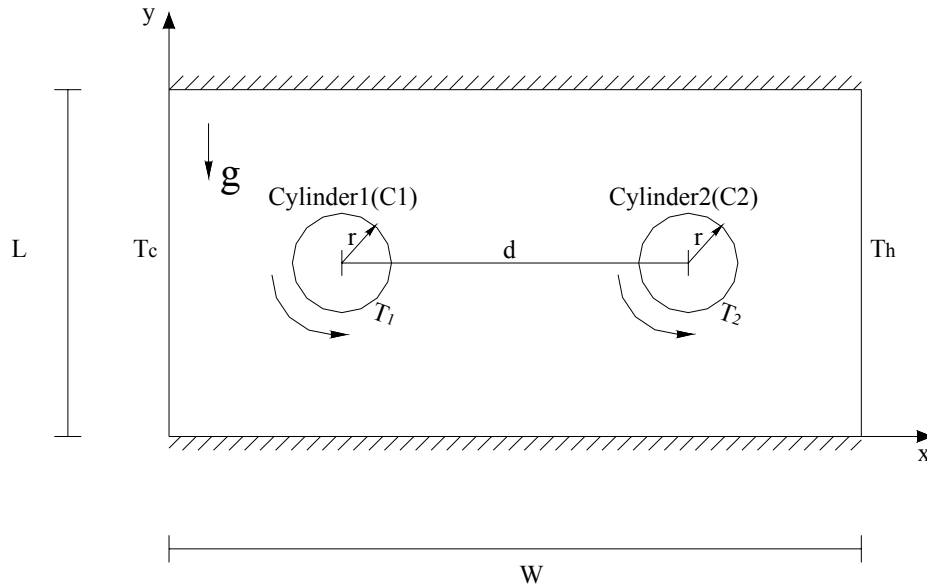


Figure 1 – Geometry and boundary conditions.

3. Problem formulation

The problem governing equations are given by the equations of mass conservation, Navier-Stokes, and energy. Being that u and v are the velocity components, T is the fluid temperature, t' is the time field, D_T is the thermal diffusivity, β_T is the thermal expansion coefficient, ν is the kinematics viscosity, g is the gravitational acceleration, ρ_0 is the fluid density and T_0 is the reference temperature taken as $T_0 = T_c$.

Under the Boussinesq approximation and the following dimensionless parameters:

$$X = \frac{x}{L}; \quad Y = \frac{y}{L}; \quad U = \frac{u}{u_{\max}}; \quad V = \frac{v}{u_{\max}}; \quad P = \frac{p}{\rho_0 u_{\max}^2}; \quad t = \frac{t'}{(L/u_{\max})}; \quad \theta = (T - T_c)/(T_h - T_c)$$

$$Fr = \frac{Re^2}{Gr}; \quad Pr = \frac{\nu}{D_T}; \quad Gr = \frac{\beta_T g \Delta T L^3}{\nu^2}; \quad Re = \frac{u_{\max} \rho_0 2r}{\mu}; \quad \Delta T = T_h - T_c; \quad A_r = \frac{L}{2r} \quad (1)$$

where Fr, Pr, Gr, Re, u_{\max} , Ar and μ are, respectively, the Froude number, the Prandtl number, the Grashof number, the Reynolds number, the velocity ($r_0 \omega$), the aspect ratio, and the dynamic viscosity, the dimensionless governing equations can be cast into the following form:

$$\frac{\partial U}{\partial X} + \frac{\partial V}{\partial Y} = 0; \quad (2)$$

$$\frac{\partial U}{\partial t} + U \frac{\partial U}{\partial X} + V \frac{\partial U}{\partial Y} = -\frac{\partial P}{\partial X} + \frac{1}{Re} \left(\frac{\partial^2 U}{\partial X^2} + \frac{\partial^2 U}{\partial Y^2} \right) \frac{1}{A_r}; \quad (3)$$

$$\frac{\partial V}{\partial t} + U \frac{\partial V}{\partial X} + V \frac{\partial V}{\partial Y} = -\frac{\partial P}{\partial Y} + \frac{1}{Re} \left(\frac{\partial^2 V}{\partial X^2} + \frac{\partial^2 V}{\partial Y^2} \right) \frac{1}{A_r} + \frac{\theta}{Fr} \frac{1}{A_r^2}; \quad (4)$$

$$\frac{\partial \theta}{\partial t} + U \frac{\partial \theta}{\partial X} + V \frac{\partial \theta}{\partial Y} = \frac{1}{Re Pr} \left(\frac{\partial^2 \theta}{\partial X^2} + \frac{\partial^2 \theta}{\partial Y^2} \right) \frac{1}{A_r}. \quad (5)$$

The boundary conditions are as follows:

$$X = 0, U = V = 0, \theta = 0, X = 2, U = V = 0, \theta = 1,$$

$$Y = 0, U = V = 0, \frac{\partial \theta}{\partial Y} = 0, Y = 1, U = V = 0, \frac{\partial \theta}{\partial Y} = 0.$$

On the cylinder surfaces: $U = \pm \sin \alpha$, $V = \pm \cos \alpha$, the temperature θ is variable.

The sign “+” or “-” depends on the rotating direction of the cylinder.

The average Nusselt number along a surface S can be written as:

$$Nu = \frac{1}{S} \int_S \frac{\partial \theta}{\partial n} ds.$$

where n means the direction perpendicular to the surface S.

In Figure 2, one can see the cases studied in this work. The cylinders C1 and C2 can be at temperatures T_c or T_h , while their surfaces may rotate with angular velocity ω in the counterclockwise (positive) and clockwise (negative) directions.

4. Solution techniques

According to Heinrich and Pepper (1999) and Donea and Huerta (2003), by applying the Petrov-Galerkin perturbations to Eqs. (2) to (5), together with the Penalty technique, the weak form of the conservation equations is as follows:

$$\int_{\Omega} N_i \left[\frac{\partial U}{\partial t} + \frac{1}{Re} \left(\frac{\partial N_i}{\partial X} \frac{\partial U}{\partial X} + \frac{\partial N_i}{\partial Y} \frac{\partial U}{\partial Y} \right) \frac{1}{A_r} \right] d\Omega + \int_{\Omega} \lambda \frac{\partial N_i}{\partial X} \left(\frac{\partial U}{\partial X} + \frac{\partial V}{\partial Y} \right) d\Omega =$$

$$\int_{\Omega} \left[(N_i + P_{il}) \left(U \frac{\partial U}{\partial X} + V \frac{\partial U}{\partial Y} \right) + N_i \sin(\gamma) \frac{\theta}{Fr} \frac{1}{A_r^2} \right] d\Omega - \int_{\Gamma_0} N_i p n_x d\Gamma \quad (6)$$

$$\int_{\Omega} N_i \left[\frac{\partial V}{\partial t} + \frac{1}{Re} \left(\frac{\partial N_i}{\partial X} \frac{\partial V}{\partial X} + \frac{\partial N_i}{\partial Y} \frac{\partial V}{\partial Y} \right) \frac{1}{A_r} \right] d\Omega + \int_{\Omega} \lambda \frac{\partial N_i}{\partial Y} \left(\frac{\partial U}{\partial X} + \frac{\partial V}{\partial Y} \right) d\Omega =$$

$$\int_{\Omega} \left[(N_i + P_{i1}) \left(U \frac{\partial V}{\partial X} + V \frac{\partial V}{\partial Y} \right) + N_i \cos(\gamma) \frac{\theta}{Fr} \frac{1}{A_r^2} \right] d\Omega - \int_{\Gamma_0} N_i p n_y d\Gamma$$

(7)

$$\int_{\Omega} \left[N_i \frac{\partial \theta}{\partial t} + \frac{1}{Re Pr} \left(\frac{\partial N_i}{\partial X} \frac{\partial \theta}{\partial X} + \frac{\partial N_i}{\partial Y} \frac{\partial \theta}{\partial Y} \right) \frac{1}{A_r} \right] d\Omega = \int_{\Omega} (N_i + P_{i2}) \left(U \frac{\partial \theta}{\partial X} + V \frac{\partial \theta}{\partial Y} \right) d\Omega$$

(8)

where $q = 0$ (no heat flux) and $p = 0$ on Γ_0 (open boundary condition – not present). The dependent variables are approximated by:

$$\Phi(X, Y, t) = \sum_j N_j(X, Y) \Phi_j(t); \quad p(X, Y, t) = \sum_k M_k(X, Y) p_k(t).$$

(9)

N_i and N_j denote the linear shape functions for Φ , that is, for U , V , and θ , and M_k denote the shape functions for the constant piecewise pressure. P_{ij} are the Petrov-Galerkin perturbations applied to the convective terms only. The terms P_{ij} are defined as follows:

$$P_{ij} = k_j \left(U \frac{\partial N_i}{\partial X} + V \frac{\partial N_i}{\partial Y} \right); \quad k_j = \frac{\alpha_j \bar{h}}{|V|}; \quad \alpha_j = \coth \frac{\gamma_j}{2} - \frac{2}{\gamma_j}; \quad \gamma_j = \frac{|V| \bar{h}}{\varepsilon_j}; \quad j=1,2$$

(10)

where γ is the element Péclet number, $|V|$ is the absolute value of the velocity vector that represents the fluid average velocity within each element, \bar{h} is the element average size, $\varepsilon_1 = 1/Re A_r$, $\varepsilon_2 = 1/Pe A_r$, P_{ij} are the Petrov-Galerkin perturbations applied to the convective terms only, α_j are the balancing diffusions, and λ is the Penalty parameter which is considered to be 10^9 . The time integration is by a semi-implicit backward Euler method. Moreover, the convective terms are calculated explicitly and the viscous and Penalty terms implicitly. The temperatures and velocities are interpolated by using the four-node quadrilateral elements and the pressure by the one-node ones. Finally, the reduced integration is applied to the penalty term to avoid numerical locking.

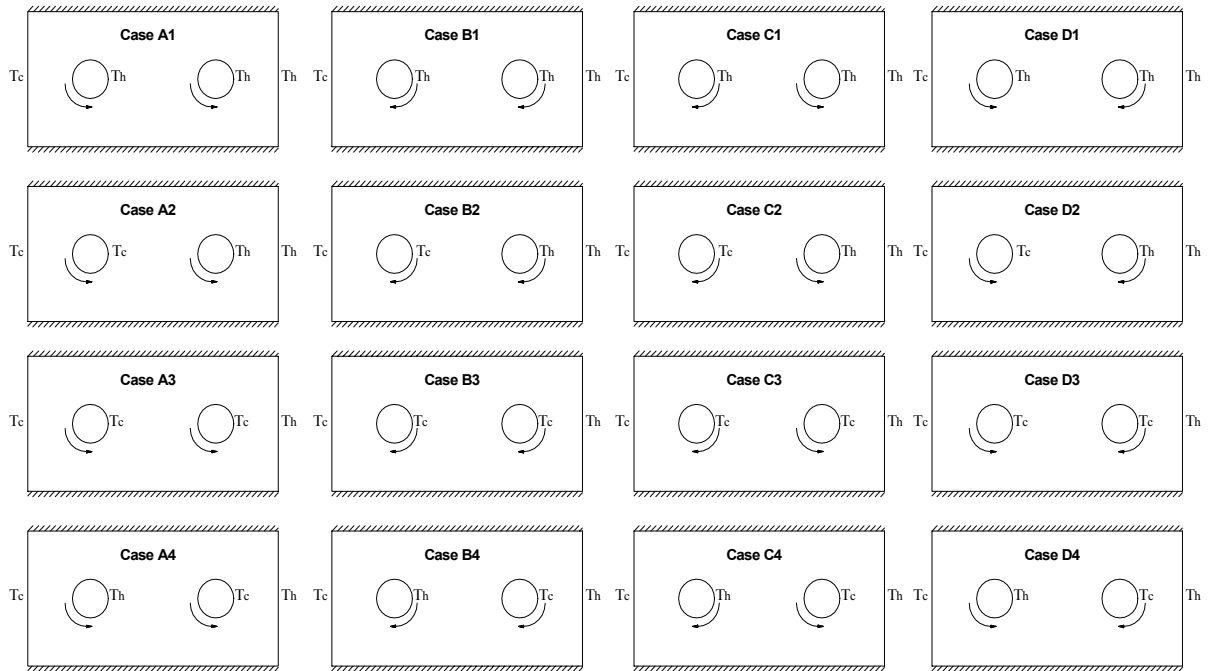


Figure 2 – Cases studied in this work.

5. Code validation

The algorithm is extensively validated by comparing the results of the present work with both the ones obtained in experimental and numerical investigations.

The first comparison is accomplished not only by using experimental results presented by Lee and Mateescu (1998) and Armaly (1983) et al., but also by numerical ones achieved by Lee and Mateescu (1998), Gartling (1990), Kim and Moin (1985), and Sohn (1988). The air flow of the present comparison analysis is taken as two-dimensional, laminar, incompressible, and under the unsteady regime. The domain is a horizontal upstream backward-facing step channel whose inlet has a fully developed velocity profile given by $u = 24y(0.5-y)\bar{U}$ and $v = 0$ in which $Re = 800$.

Table 1 shows the results for the first comparison among the flow separation distances X_s and the flow reattachment distances X_{rs} on the upper surface. As for the bottom surface, the reattachment distances X_r are compared. H_d and H_u are the channel downstream and upstream heights, respectively. As it can be noticed, the results of the present work agree well with the ones from the literature.

Table1: Results for the first comparison.

		Experimental results			Computed results			
		Lee and Mateescu (1998)	Armaly et al. (1983)	Present prediction	Gartling's prediction (1990)	Kim & Moin (1985)	Lee and Mateescu (1998)	Sohn (1988)
Length on								
Lower Wall	x_r	6.45	7.0	5.75	6.1	6.0	6.0	5.8
Upper Wall	x_s	5.15	5.7	4.95	4.85	-	4.8	-
	x_{rs}	10.25	10.0	9.9	10.48	-	10.3	-
	$x_{rs}-x_s$	5.1	4.3	4.95	5.63	5.75	5.5	4.63
Reynolds		805	800	800	800	800	800	800
Hd/Hu		2	1.94	2	2	2	2	2

The second comparison is performed with the numerical results shown by Comini (1997) et al. The contrasting study is carried out by considering a Poiseuille flow in a horizontal channel heated from below. Some values are chosen such as $Re = 10$, $Pr = 0.67$, and $Fr = 1/150$. The grid has 4000 quadrilateral four-node elements with $\Delta x = 0.1$, $\Delta y = 0.15$, $\Delta t = 0.01$ and 1000 iterations. The average Nusselt number on the upper surface is 2.44. This value agrees satisfactorily with the one found by Comini (1997) et al. which is 2.34, featuring a deviation of about 4%.

Concluding the comparison, the third case studied to validate the mathematical modeling code involves mixed convection of air between two horizontal concentric cylinders with a cooled rotating outer cylinder. Some parameters are considered such as: $Pr = 0.7$, $Re = 10, 50, 100, 150, 200, 250, 300, 350$, and 500 , and $Ra = 10^4, 2 \times 10^4$, and 5×10^4 . The domain is spatially discretized with 5976 non-structured four-node quadrilateral elements.

The values are compared to the ones found in Yoo (1998). They use a grid (radial x angular) of (65×64) points and a finite difference scheme. The results from the present work against to the ones in Yoo (1998) can be seen in Fig. 3. Although the results found in third comparison are higher than the ones in Yoo (1998), it is interesting to note the similar behavior of the two curves. The authors think it is relevant to show this comparison since some future works on numerical methods may use these data for comparison. The time step used is 0.01 for almost all cases which are run in the present work, and the number of iterations ranges from 10^4 to 3×10^4 .

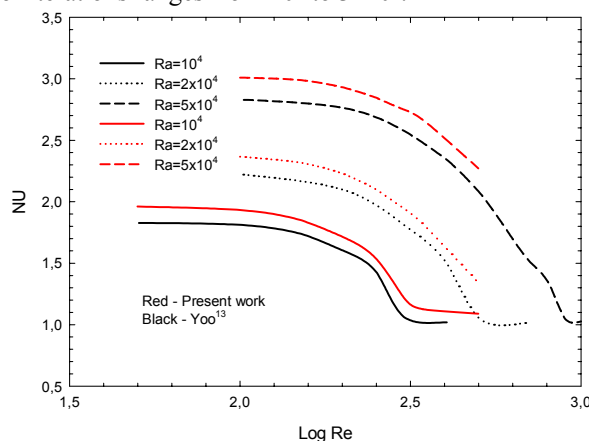


Figure 3: Comparison of overall average Nusselt number for the third comparison.

6. Results

A study of convergence of mesh refinement with 5926 and 8176 elements is carried out.

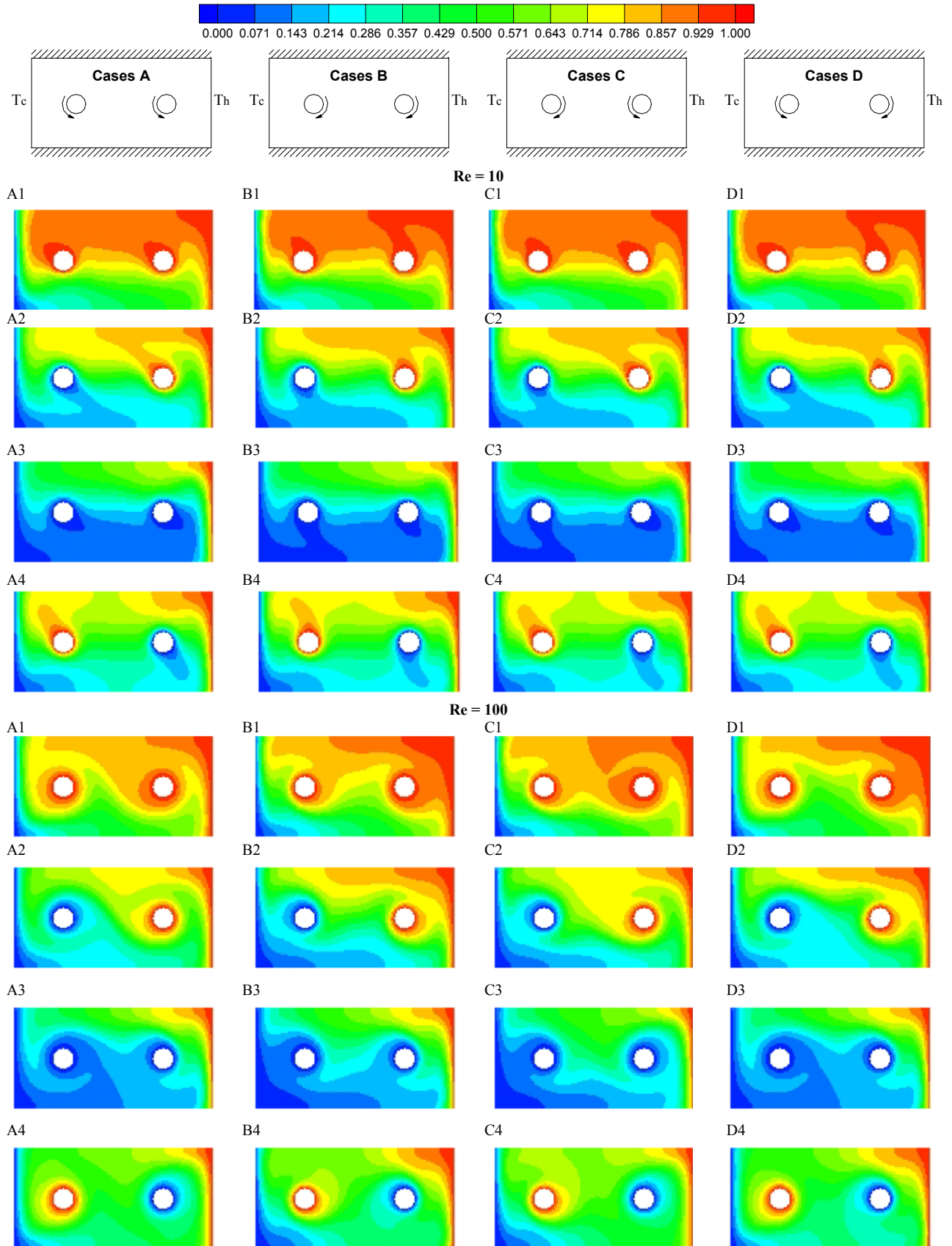


Figure 4 – Isotherms for $Re = 10, 100$ and $Gr = 10^5$.

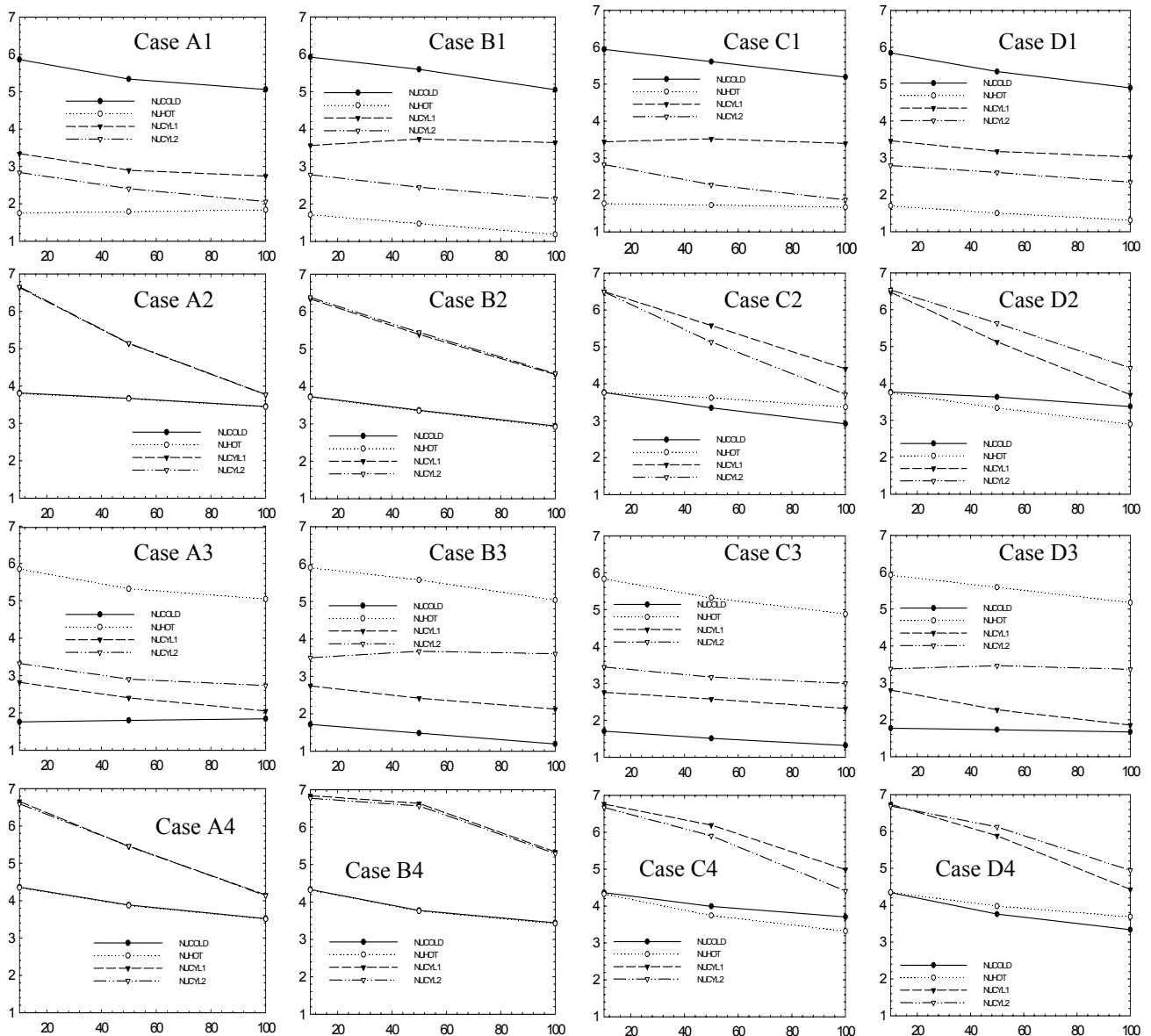


Figure 5 – Average Nusselt numbers for cases from Fig. 2 versus Reynolds numbers

For both meshes, the time increments are: $\Delta t = 0.01$ for $Gr = 10^3$ and 10^4 . For $Gr = 10^5$, when the mesh has 5926 elements, $\Delta t = 0.005$ and for 8176 elements, $\Delta t = 0.001$, in general. The mesh with 8176 elements is chosen to run all the cases from Fig. 2 with a maximum deviation of 1.9%. The cases from Fig. 2 are studied considering Grashof number $Gr = 10^5$ and Reynolds numbers $Re = 10, 50, 100$, and 500 . In Fig. 4, the temperature distributions are shown only for $Gr = 10^5$ and $Re = 10$ and 100 , considering cases A, B, C, and D. When $Re = 10$, the buoyancy forces are more dominant over the velocities of the cylinders. Whatever the angular velocity direction is for $Re = 10$, the isotherms do not seem to change significantly if the cylinder temperatures are not changed. However, for $Re = 10$, if the cylinder velocity directions do not vary, the temperature imposed at the cylinder surfaces play quite an important role on the isotherms and, hence, on the heat transfer. On the other hand, when $Re = 100$, which means higher velocities on the cylinder surfaces, the directions of the angular velocities influence more significantly on the temperature distributions when the cylinder temperatures are kept the same. Figure 5 presents the average Nusselt number along the cold (NUCOLD), hot (NUHOT), cylinder 1 (NUCYL1), and cylinder 2 (NUCYL2) surfaces, where $Gr = 10^5$ and $Re = 10, 50$, and 100 . The case sets (A1...D1), (A2...D2), (A3...D3), and (A4...D4) represent the influence of the direction only. While the sets (A1...A4), (B1...B4), (C1...C4), and (D1...D4) denote the cylinder surface temperature variation only. Many results can be brought up from Figs. 5. However, just few of them will be mentioned. In case B4, one can note a strong influence on heat transfer for $Re = 50$ and 100 compared to A4. It is also worth observing the coincidence of Nusselt number in (A2, B2). In addition, in (C2, D2) and (C4, D4) there are inversions of the Nusselt number behavior. In C2, $NUCYL1 > NUCYL2$ and $NUHOT > NUCOLD$. In D2, $NUCYL1 < NUCYL2$ and $NUHOT < NUCOLD$.

7. Conclusion

It is studied in this work the natural convection within an enclosure with two internal heated cylinders considering the regime two-dimensional and unsteady. The Prandtl number is $Pr = 0.7$ and the Grashof number is $Gr = 10^5$ throughout this research. Just one comparison is carried out. The geometry considered is a two-concentric cylinder enclosure where the outer one is cooled and rotating while the inner one does not rotate and is heated. It has been found that a mesh with 8176 elements provides an acceptable convergence in the mesh refinement study. The governing equations are discretized using the finite element method with the Petrov-Galerkin perturbations applied to the convective terms and the Penalty formulation to the pressure terms. A semi-implicit Euler method is used to advance in time. The computational code is run in a PC Pentium 4, processor running at 2.8 Ghz and 512 of RAM. In fact, a variety of results is reached here. However, what is worth mentioning is that the cylinder direction is really important when high angular velocities are present. This is a situation that controls the main flow. Indeed, there are some cases which should be avoided when cooling is aimed, that is, the ones with high temperatures.

8. Responsibility notice

The authors are the only responsible for the printed material included in this paper.

9. Acknowledgements

The authors acknowledge CAPES for the financial support without which this study would be impossible.

10. References

- Armaly, B. F., Durst, F., Pereira, and J. C. F. & Schonung, B., 1983. Experimental and Theoretical Investigation of Backward-Facing Step Flow, *Journal of Fluid Mechanics*, vol. 127, pp. 473-496.
- Comini, G., Manzam, M. and Cortella, G., 1997. Open Boundary Conditions for the Streamfunction-Vorticity Formulation of Unsteady Laminar Convection, *Numerical Heat Transfer*, Part B, vol. 31, pp. 217-234.
- Fu, W.S., Cheng, C.S. and Shieh, W.J., 1994. Enhancement of Natural Convection Heat Transfer of an Enclosure by a Rotating Circular Cylinder, *Int. J. Heat Mass Transfer*, vol. 37, No. 13, pp. 1885-1897.
- Gartling, D. K., 1990. A Test Problem for Outflow Boundary Conditions – Flow over a Backward-Facing Step, *International Journal of Numerical Methods in Fluids*, vol. 11, pp. 953-967.
- Kim, J. and Moin, P., 1985. Application of a Fractional-Step Method to Incompressible Navier-Stokes Equations, *Journal of Computational Physics*, vol. 59, pp. 308-323.
- Lee, J., Kang, S. H. and Son, Y. S., 1999. Experimental Study of Double-Diffusive Convection in a Rotating Annulus with Lateral Heating, *Int. J. Heat Mass Transfer*, vol. 42, pp. 821-832.
- Lee, T. and Mateescu, D., 1998. Experimental and Numerical Investigation of 2-D Backward-Facing Step Flow, *Journal of Fluids and Structures*, vol. 12, pp. 703-716.
- Lin, D. and Yan, W.M., 2000. Experimental Study of Unsteady Thermal Convection in Heated Rotating Inclined Cylinders, *Int. J. Heat Mass Transfer*, vol. 43, pp. 3359-3370.
- Nguyen, H. D., Paik, S. and Douglass, R. W., 1996. Unsteady Mixed Convection About a Rotating Circular Cylinder with Small Fluctuations in the Free-Stream Velocity, *Int. J. Heat Mass Transfer*, vol. 39, No. 3, pp. 511-525.
- Sohn, J., 1998. Evaluation of FIDAP on Some Classical Laminar and Turbulent Benchmarks, *International Journal of Numerical Methods in Fluids*, vol. 8, pp. 1469-1490.
- Yoo, J., 1998. Mixed Convection of Air Between Two Horizontal Concentric Cylinders with a Cooled Rotating Outer Cylinder, *Int. J. Heat Mass Transfer*, vol. 41, No. 2, pp. 293-302.